Wang *et al.*
European Journal of Medical Research (2025) 30:347
https://doi.org/10.1186/s40001-025-02619-y

European Journal of Medical Research

RESEARCH

Open Access

LPM electrode loaded with RAPA-PLGA drug sustained-release system can reduce local fibrous tissue hyperplasia and local bioelectrical impedance

Xiu Wang[1], Wentao Du[2*], Yunyun Wang[1], Ahsan Riaz Khan[3,4] and Haijun Zhang[1,3,4,5*]

Abstract

Objective This study aims to design and fabricate a leadless pacemaker (LPM) electrode loaded with rapamycin (RAPA)–poly(lactic-co-glycolic acid) (PLGA) drug sustained-release system to reduce the local fibrous tissue proliferation after LPM implantation, reduce local bioelectrical impedance, and facilitate the safe extraction of LPM after use.

Methods We fabricated an LPM electrode loaded with the RAPA-PLGA drug-sustained-release system and carried out in vitro and in vivo experiments to verify its effect.

Results A scanning electron microscope showed that the LPM electrode cavity was loaded with the RAPA-PLGA drug's sustained-release system. The energy-dispersive spectrometer showed that the LPM electrode had RAPA and PLGA-related elements. The average drug loading rate of the drug sustained-release system was (51.02% ± 2.66) %, and the encapsulation rate was (85.04% ± 4.43%). The RAPA loaded in the electrode chamber was about (337.83 ± 53.66)μg. In vitro release results show that the LPM electrode loaded with RAPA–PLGA can continue to release for 44 days. In vitro cell inhibition experiments showed that the drug-loaded electrode group had an obvious inhibitory effect on fibroblasts, and the difference between the groups was significant ($p < 0.05$). In vivo experiments showed that the local bioelectrical impedance of the drug-loaded electrode group is lower than that of the control group, with a difference between groups with statistical significance ($p < 0.05$). The histopathological analysis of tissue sections from the site of (LPM electrode implantation revealed reduced fibrous tissue hyperplasia in the drug-loaded electrode group compared to the control group. Additionally, H&E staining indicated that the implantation of drug-loaded electrodes did not induce abnormal alterations in the liver, heart, spleen, lung, or kidney tissues.

Conclusion The LPM electrode loaded with RAPA–PLGA demonstrates significant, sustained drug release and antiproliferative effects in vitro. This drug-loaded electrode has been deemed safe for implantation in animal models. It can effectively inhibit local fibrous tissue proliferation and reduce local bioelectrical impedance, offering a technical strategy to prolong the in vivo functionality of LPMs and enhance clinical procedures.

Keywords Leadless pacemakers, Electrode, Rapamycin, PLGA, Fibrous tissue hyperplasia

*Correspondence:
Wentao Du
1961147104@qq.com
Haijun Zhang
zhanghaijun@tongji.edu.cn
Full list of author information is available at the end of the article

Introduction

Bradyarrhythmia is an arrhythmia with a ventricular rate lower than 60 beats per minute, which mainly occurs in the elderly. The incidence of bradyarrhythmia is rising annually due to the aging population. The installation of a permanent cardiac pacemaker is the initial and most effective treatment for symptomatic bradyarrhythmia. Leadless pacemakers (LPM) can avoid complications, such as lead- and pock-related infection and lead fractures of traditional transvenous pacemakers [1, 2], and have achieved good clinical application. However, the long-term pathological results of LPM implantation show that there is local fibrous tissue proliferation in the myocardial tissue of the LPM implantation site, which affects the use of a pacemaker and the safety of LPM extraction [3, 4].

Rapamycin (RAPA) is a new macrolide anti-rejection drug, which was approved by the FDA as an immunosuppressant in 1999. Because of its good immune effect and wide safe dose range, it is widely used in anti-rejection of organ transplantation and the treatment of autoimmune disease [5, 6]. Numerous malignancies are treated with RAPA due to its anticancer efficacy and low toxicity [7, 8]. Studies on RAPA in the field of cardiovascular medicine have proven that RAPA can prevent vascular smooth muscle from proliferating and vascular intima from becoming hyperplasia. RAPA received approval in 2003 to be used in drug-eluting stents to stop vascular restenosis following stent insertion [9]. In addition, many studies indicate that RAPA can improve heart function and lessen the infarction area in rats following myocardial infarction and left ventricular remodeling [10]. It can also alleviate myocardial fibrosis caused by cardiomyopathy in rats [11] and has a therapeutic effect on liver, pulmonary, and kidney fibrosis [12–14].

Poly(lactic-co-glycolic acid) (PLGA) is a polymer compound formed by the polymerization of polylactic acid and glycolic acid. In in vivo, PLGA can hydrolyze into lactic acid and glycolic acid. It can then be further metabolized through the tricarboxylic acid cycle to produce carbon dioxide and water, which is then expelled into the lungs. It is extensively employed as a drug-controlled release carrier for the treatment of disorders because of its strong biocompatibility and degradability [15, 16], the related nano-drug delivery system has also attracted much attention [17, 18].

However, there is no effective strategy to solve the local proliferation complications caused by LPM implantation, and there are also no relevant studies that load drug sustained-release systems on LPM. Therefore, this study aims to develop a RAPA–PLGA sustained-release system for LPM electrodes, followed by comprehensive characterization, including morphological evaluation, in vitro drug release profiling, cellular inhibitory assessment, and in vivo performance analysis. These investigations seek to provide novel strategies for mitigating local complications associated with LPM implantation.

Materials and methods

Materials

Poly(D-, L-lactic-co-glycolic) (PLGA, 50:50, viscosity 0.38 dL/g, Av. Mw 40,000) with an ester end group was purchased from Shandong Institute of Medical Instrument (Shandong, China). Rapamycin (Sirolimus, 98% purity), Methanol, acetonitrile (chromatographic grade), 10% sodium dodecyl sulfate (SDS) solution, and benzoyl peroxide were purchased from Macklin Biochemical Technology Co., Ltd. (Shanghai, China). The leadless pacemaker electrodes were provided by Shandong Rientech Medical Technology Co., Ltd. (Dezhou, China). Dichloromethane, ethanol absolute, and xylenes were supplied by Sinopharm Chemical Reagent Co., LTD. (Shanghai, China). Dulbecco's modified Eagle medium (DMEM), sterile phosphate-buffered saline (PBS), dimethyl sulfoxide (DMSO, ACS grade), penicillin–streptomycin, 0.25% trypsin, fetal bovine serum (FBS) was purchased from Thermo Fisher Scientific (Massachusetts, USA). The Cell counting Kit–8 was purchased from Proteintech Group, Inc. (Chicago, USA). Xylazine hydrochloride was purchased from Jilin Province Huamu Animal Health Products Co., LTD. (Jilin China). Methyl methacrylate and dibutyl phthalate were purchased from Shanghai Aladdin Biochemical Technology Co., LTD. (Shanghai, China). HE staining solution (kit) was purchased from Beijing Solarbio Science & Technology Co., Ltd. (Beijing, China).

Microbalance (MX5) was purchased from Meltlier-Toledo International Inc. (Ohio, USA). The vacuum-drying machine (DFZ) was bought from Lichen Instrument Technology Co., LTD. (Shanghai, China). The air bath thermostat oscillator (SHZ-82 A) was purchased from Shaoxing Supo Instrument Co., LTD. (Shaoxing, China). A digital ultrasonic cleaning machine was bought from Jeken Ultrasonic Equipment Co., LTD. (Dongguan, China). The HPLC instrument (LC-20 AD_{XR}) was purchased from Shimadzu Corporation (Kyoto, Japan). Cell incubator and magnetic stirring were bought from Yiheng Scientific Instrument Co., Ltd. (Shanghai, China). The labeled instrument was purchased from BioTek Instruments, Inc. (Vermonte, USA). An electrochemical workstation was purchased from Ametek Inc. (Pennsylvania, USA). The embedding machine and the embedding machine cooling table were purchased from Rayto Life and Analytical Sciences Co., Ltd. (Shenzhen, China). Microtome was purchased from Leica (Wetzlar, Germany). Hard sectioning microtom was

purchased from Xi'an Lanming Medical Technology Co., LTD (Xian, China).

NCTC clone 929 cells were bought from Rocell Life Science & Technology Co., Ltd. (Wuhan, China).

LPM electrode loaded RAPA–PLGA drug sustained-release system and morphological characterization

The RAPA–PLGA drug sustained-release system was put into the LPM electrode cavity after being manufactured using the organic solvent evaporation method. Science 200 mg of PLGA was weighed and added to 5 ml dichloromethane, and the mixture was further ultrasonically mixed with 300 mg of RAPA. The system was then constantly stirred for four hours using a magnetic stirring apparatus in the fuming cupboard in order to exclude volatile organic solvent fuming, further dehydration of the organic solvents,, the RAPA–PLGA drug sustained-release was injected into the LPM electrode cavity, and moved to the vacuum-drying oven for three days to exclude organic solvent completely. At this point, the RAPA–PLGA drug sustained-release system was loaded onto the LPM electrode; through the opening of the electrode cavity surface, contact between the drug sustained-release system and the local tissue can be achieved to play a role of drug sustained-release (Fig. 1A–C).

Three LPM electrodes with and without a drug sustained-release system loaded with RAPA–PLGA and were removed and vacuum-dried. An energy-dispersive spectrophotometer (EDS) was used to investigate the surface element distribution, and scanning electron microscopy (SEM) was used to examine the shape of LPM electrodes both before and after drug loading.

Determination of RAPA

Drawing of the standard curve of RAPA

10 mg of RAPA was dried under reduced pressure and precisely weighed to constant weight acetonitrile in a 100-volumetric flask. Acetonitrile was added to a constant volume of 100 ml. 100 $\mu g \cdot ml^{-1}$ RAPA standard sample stock solution was obtained after ultrasonic mixing. With the RAPA stock solution diluted to 10–100 $\mu g \cdot ml^{-1}$ ($n \geq 5$) and 0.1–10 $\mu g \cdot ml^{-1}$ ($n \geq 5$), high-performance liquid chromatography (HPLC) was used to quantify the absorption peak area. The concentration (C) served as the abscissa, the peak area of the sample (Y) as the ordinate, and the regression curve was created. The standard curve equation is generated using the linear regression equation.

Chromatographic conditions

WondaSil-C18 column (4.6 mm ×150 mm, 5 μm, S/N:6L5503-22), Mobile phase:methanol:water (v/v) =75:25 [19], Detection wavelength: 277 nm, Velocity: 1 $ml \cdot min^{-1}$, column temperature: 50 ℃, Injection volume: 20 μL.

Method specificity

Taking the RAPA standard solution, respectively, the extracted solution of LPM electrode loaded with RAPA–PLGA drug sustained-release system, and blank 0.3% SDS

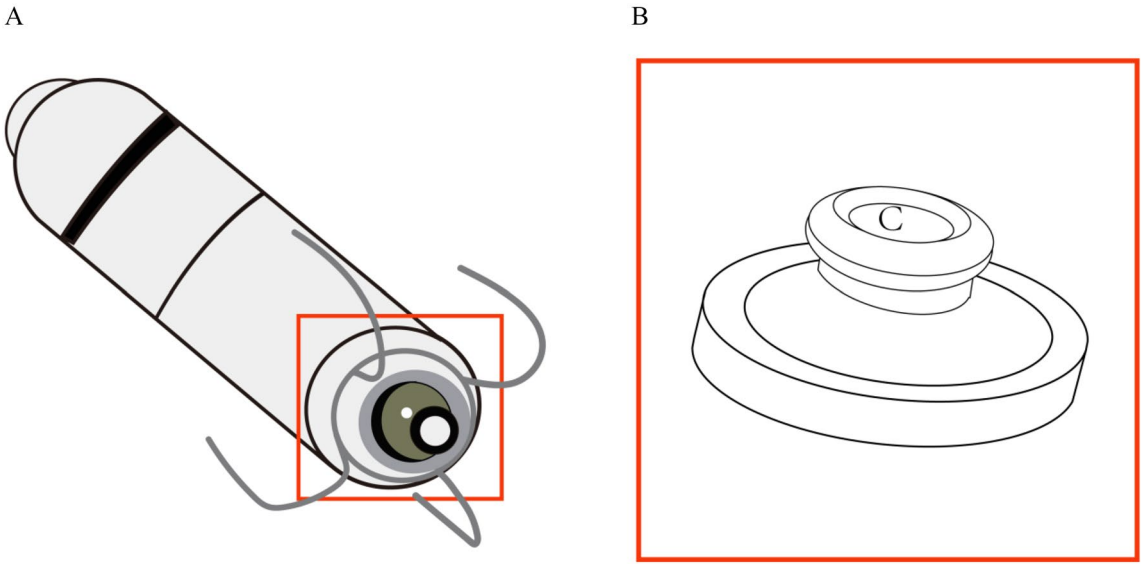

Fig. 1 Schematic of leadless pacemaker electrode tip architecture. **A** Schematic representation of leadless pacemaker, **B** The head of Leadless pacemaker, **C** The electrode cavity of leadless pacemaker

solution 20 μL, using the methods shown in 2.3.2 sample, record chromatograph chart to examine the specificity of the detection method.

Precision, accuracy, and method recovery

Respectively prepared mass concentration of 50 $\mu g \cdot ml^{-1}$, 5 $\mu g \cdot ml^{-1}$ and 0.5 $\mu g \cdot ml^{-1}$ RAPA high, medium, and low are three kinds of reference substance solutions. The chromatographic conditions shown in 2.3.2 were used for sample injection analysis. Intra-day precision (intra-RSD) and accuracy were calculated by repeated measurement three times within one day, and inter-day precision (inter-RSD) and accuracy were calculated for three consecutive days. To figure out the RAPA content, the measured peak area was inserted into the standard curve. The computed value was then divided by the known content to determine the required recovery rate.

Stability of RAPA in the release medium

Three samples of 0.3% SDS solution with RAPA mass concentration of 5 $\mu g \cdot ml^{-1}$ were prepared and placed at (37 ± 1) ℃, the chromatographic conditions as shown in 2.3.2 were used for sample analysis at 1 day, 3 days, 5 days, and 8 days, respectively. In order to determine the RAPA content and recovery rate, the measured peak area was substituted into the standard curve, and the stability of RAPA in a 0.3% SDS solution was examined.

Drug-loading rate and Encapsulation efficiency determination

Three aliquots of 5 mg RAPA–PLGA drug sustained-release systems prepared at different time points were individually solubilized with 20 mL acetonitrile under vortexing for complete dissolution. The solution was placed in an air bath with a constant temperature oscillator at 37 ± 1 ℃, shaken at 100$r \cdot min^{-1}$ for 6 h, mixed by ultrasound for 30 min, filtered by 0.22 μm filter membrane, and injected for analysis according to the chromatographic conditions shown in 2.3.2. The peak area was recorded and replaced into the linear regression equation to calculate the drug content of RAPA. DL rate and EE were calculated according to the following Eqs. (1 and 2).

$$\mathrm{DL}\ (\%) = \frac{\text{Mass of RAPA in the RAPA} - \text{PLGA}}{\text{Mass of the RAPA} - \text{PLGA}} \times 100 \tag{1}$$

$$\mathrm{EE}\ (\%) = \frac{\text{Mass of RAPA in the RAPA} - \text{PLGA}}{\text{Mass of RAPA theoretical}} \times 100 \tag{2}$$

RAPA content loaded in the LPM electrode

The microelectronic balance MX5 was used to weigh the mass of 32 LPM electrodes loaded with the RAPA-PLGA drug sustained-release system before and after drug loading to determine the actual mass of the RAPA–PLGA drug sustained-release system. According to the determination of the DL rate calculated in 2.5, RAPA theory content in the electrode was figured out by Eq. (3) where $RAPA_{throry}$ is the theoretical content of RAPA in the electrode, M_{after} is the mass of electrode after loaded RAPA-PLGA, M_{before} is the mass of electrode before loaded RAPA-PLGA.

$$\mathrm{RAPA_{theory}} = (\mathrm{M_{after}} - \mathrm{M_{before}}) * \mathrm{DL}(\%) \tag{3}$$

The in vitro release of LPM electrode loaded with RAPA-PLGA drug sustained-release system

Three LPM electrodes loaded with RAPA–PLGA drug sustained-release system were used, and 5 ml of 0.3% SDS solution with pH of about 7.4 was used as the release medium of rapamycin (SDS surfactant was added to the water to regulate the drug release rate and meet the blood pH use environment). The in vitro release system of each group was placed in an air bath with a a constant temperature of 37℃ and oscillator; frequency of (75 ± 15) $r \cdot min^{-1}$. The release medium was replaced with a fresh medium at predetermined time intervals of (1, 3, 5, 8, 15, 22, 30, 37, 41, and 44 days) following sample extraction. RAPA content was determined using the chromatographic conditions described in 2.3.2. The cumulative release rate was calculated from Eqs. (4 and 5), where Q_n is the accumulative drug release mass, V_i is the volume of the withdrawn medium, C_i is the drug concentration in the release medium at each time point, and W is the total drug content of the release sample.

$$\mathrm{Q_n} = \sum_{i=0}^{n-1} C_i V_i \tag{4}$$

$$\text{Cumulative release rate}(\%) = \mathrm{Q_n}/\mathrm{W} \times 100 \tag{5}$$

Cell inhibition effect of LPM electrode loaded with RAPA–PLGA drug sustained-release system in vitro

The Cell Counting Kit-8 (CCK-8) assay was utilized to evaluate the cell inhibition effect of the LPM electrode loaded with the RAPA–PLGA drug sustained-release system on NCTC clone 929 cells. The experimental groups were as follows: the LPM loaded with RAPA–PLGA group (one LPM electrode loaded with RAPA–PLGA drug sustained-release system in 5 ml complete medium (DMEM medium with 10% FBS and 1% penicillin–streptomycin) with 0.2% dimethyl sulfoxide (DMSO), the LPM blank electrode group (one LPM blank electrode in 5 ml complete medium with 0.2% DMSO), positive control

(0.5 ml DMSO in 4.5 ml complete medium), negative control (1 g high-density polyethylene in 5 ml complete medium), and blank control (complete medium only). Samples from these different groups were extracted and stored in a 4 ℃ refrigerator. The extracts collected on the first, third, and seventh days and then co-cultured with cells to assess the in vitro cell inhibition effect of the drug-loaded electrodes. For cell culture, the NCTC clone 929 cells were cultured in a complete medium and placed in a 37 ℃ incubator with 5% CO_2. Cells in the logarithmic growth phase were detached using 0.125% trypsin to create a single-cell suspension with a cell density of 4×10^4 cells·ml^{-1}. These cells were then seeded onto a 96-well plate with 100 μL per well. After 24 h of culture and reaching 90% confluence, the previous medium was removed, and the appropriate extract was added according to the respective group. Following a 48-h co-culture, a complete medium with CCK-8 reagent was added to each well. After 1–4 h of incubation, the optical density (OD) at 450 nm was measured using an enzyme-linked instrument and compared across groups. Cell viability (%) was calculated using the formula provided, where A_s represents the experimental well (medium containing cells and tested substances, CCK-8), A_b is the blank well (medium containing CCK-8 without cells or tested substances). Ac is the control well (medium containing cells and CCK-8 without the test substance).

$$\text{Cell inhibition rate (\%)} = (A_c - A_s)/(A_c - A_b) \times 100\% \quad (7)$$

In vivo experiments of electrodes loaded with RAPA-PLGA

Animals and groups

Kunming mice with SPF grade were selected for the in vivo experiment, which was purchased from Jinan Pengyue Experimental Animal Breeding Co., LTD., qualification certificate number: SCXK (Lu) 20,220,006, a total of 6 mice, 12 weeks old, half male and half female, weight 30 ± 5 g. The experimental animals were raised in Shandong Anzhong Medical Equipment Inspection and Testing Co., LTD., license certificate number SYXK (Lu) 20,230,010. The experiment was approved by the Animal Ethics Committee Ethics Review No. (04) 2023 of Shandong Anzhong Medical Device Inspection and Testing Co., LTD. The mice were randomly divided into two groups: the experimental group was implanted with LPM electrodes loaded with RAPA–PLGA drug sustained-release system, and the control group was implanted with blank LPM electrodes, with 3 mice in each group.

Implantation of LPM electrode and determination of local bioelectrical impedance

The implantation experiment was carried out after 2 weeks of adaptive feeding. Since the mice were anesthetized with xylazine hydrochloride, the electrodes were loaded with the RAPA–PLGA drug sustained-release system, and blank electrodes were implanted into the muscle tissue of the legs of the corresponding mice. An electrochemical workstation was used to measure the local bioelectrical impedance among them. WE + SE is the first electrode, and the second electrode is CE + RE. The electrode probe head adopts two stainless steel conductive wires with a diameter of 1 mm, and the middle one is fixed with non-conductive polyamide so that the spacing between the two electrode needles remains 0.8 cm (Fig. 4B). After implantation of two months, mice were anesthetized with xylazine hydrochloride, and the skin at the electrode implantation site was cut open. Then, electrode probes were pierced in on either side of the electrodes implanted, with a depth of 0.5 cm. The Versa Studio software was used to measure the, spectral range (30 kHz–1000 kHz) frequencies to measure and record the impedance spectra corresponding for subsequent analysis.

Sample collection and hematoxylin–eosin (H&E) staining

After the measurement of the lung's local bioelectrical impedance of different electrodes, muscle tissue samples containing electrodes and internal organs, such as liver, heart, spleen, lung, and kidney, were collected. Specimens were fixed with tissue fixative wax for 48 h and dehydrated. The organ specimens were infiltrated and embedded with paraffin, and the local tissues at the electrode implantation site were infiltrated and embedded with methyl methacrylate, dibutyl phthalate, and benzoyl peroxide. Pathological sections from the above-embedded samples were made, and the tissue pathology status was observed through H&E staining.

Statistical analysis

SPSS 25.0 and GraphPad Prism 8 software were used for statistical analysis. Numerical variables with normal distribution were described as ($\overline{X}$ ± S), and categorical variables were described as the number of cases (n) and its percentage (%). The relationship between RAPA concentration and peak area was analyzed using simple linear regression, and $R^2 \geq 0.99$ indicates a good linear relationship. The difference between LPM loaded with RAPA–PLGA drug sustained-release system and other groups was analyzed by one-way ANOVA, one-way ANOVA analyzed the other groups. The LSD-t test was used for pairwise comparisons with a statistical difference. $p < 0.05$ was considered as statistical significance.

Results

Morphological characterization of LPM electrode loaded RAPA-PLGA drug

Following the integration of RAPA-PLGA drug-sustained system onto the LPM electrode, the electrode cavity became completely filled with the drug-sustained system. The RAPA-PLGA coated electrode surface exhibited relatively smooth and uniform with the drug-sustained layer remaining in direct contact with the external environment (Fig. 1A, B).

The molecular formula of RAPA is $C_{51}H_{79}NO_{13}$, the molecular formula of PLGA is: $(C_3H_4O_2)_{50}(C_2H_2O_2)_{50}$, EDS scanning of the surface of LPM electrode after loading RAPA-PLGA drug sustained-release system showed the existence of elements associated with RAPA and PLGA, preliminarily indicating that the drug release system was successfully loaded (Fig. 2C–E).

The standard curve of RAPA

RAPA was well-separated from other substances under the chromatographic conditions as described 2.3.2, and the lowest detection limit was 0.1 μg·ml^{-1}. Due to the large concentration span in the process of drug detection, two sets of standard curves were drawn. The peak area (Y) was used for linear regression of the mass concentration (C, μg·ml^{-1}), and the regression equation of 0.1–10 μg·ml^{-1} was obtained: Y= 48281 C-1948.5, R^2= 0.9994, the regression equation of 10–100 μg·ml^{-1} regression equation was: Y= 54986 C–80,387, R^2= 0.9999. The results showed that the RAPA had a good linear relationship with the peak area in the concentration range of 0.1–10 μg·ml^{-1} and 10–100 μg·ml^{-1} (Fig. 3A, B).

Specificity of the method

No interference peak was found at the peak location of the blank 0.3%SDS solution and other electrode substances with the RAPA-PLGA drug sustained-release system during the detection of RAPA. The retention time of the sample solution and the standard solution of rapamycin in the chromatogram was similar, and both peaked within 32 ±1 min. Results show that the measurement method technique has good specificity (Fig. 3C).

Precision, accuracy, and method recovery

Intra-RSD, inter-RSD, accuracy, and method recovery rate were tested according to the above method. Intra-RSD fluctuated between 0.42% and 2.73% (Table 1), inter-day precision fluctuated between 2.67% and 2.83% (Table 2), accuracy ranged from 0.53% to 4.73%, and average recovery was 95–105% (Table 3). These findings demonstrated that the intra-day and inter-day errors of the measurement method were modest and within practicable limits. Thus, the RAPA content was precise and reliable method.

Stability of RAPA in release medium

In order to investigate the stability of RAPA in the release medium, RAPA was dissolved in 0.3%SDS solution to 5 μg·mL^{-1} and placed at (37 ±1) ℃ for eight days. The recovery of RAPA on the 1 st and 8 th day 1 was (100.06 ± 3.57) % and (95.24 ± 3.85) %, respectively (Table 4). These results indicated that RAPA was stable in 0.3%SDS solution for at least 8 days. Therefore, the longest single extraction time of the drug-loaded electrode was ≤ 8 days to ensure the accuracy of RAPA content during the in vitro release effect study.

Drug-loading (DL) rate and encapsulation efficiency (EE)

Using the method of 2.6, we detected the DL rate and EE of three RAPA–PLGA sustained-release systems made at different times. Our results revealed that the average DL rate was (51.02 ± 2.66)%, and the average EE was (85.04 ± 4.43)% (Table 5).

Drug content of each drug-loaded electrode

The average reduced mass of 32 LPM electrodes before and after being loaded with RAPA-PLGA drug sustained-release system, that is, the mass of RAPA-PLGA loaded on the electrode was (662.16 ± 105.18) μg. According to Eq. (3), we can know that the average RAPA drug content ($RAPA_{theory}$) loaded on the electrode was (337.83 ± 53.66) μg.

The release effect of LPM electrode loaded with RAPA-PLGA drug sustained-release system in vitro

The results of in vitro release showed that the cumulative drug release rate of LPM electrodes loaded with RAPA-PLGA drug sustained-release system was (14.78 ± 3.25) % in the first day, (15.40 ± 2.59) % in the first 3 days (16.64 ± 6.26) % in the first 8 days. The drug was released stably within 1 month, and the cumulative release rate of the drug was (30.97 ± 5.86) %. The RAPA-PLGA drug sustained-release system in the LPM electrode began to disintegrate with a large amount of drug release at about 37 days; the medication release was essentially finished after 44 days, and the cumulative drug release could reach 30% of the total drug content at 37 days to 44 days (Fig. 3D).

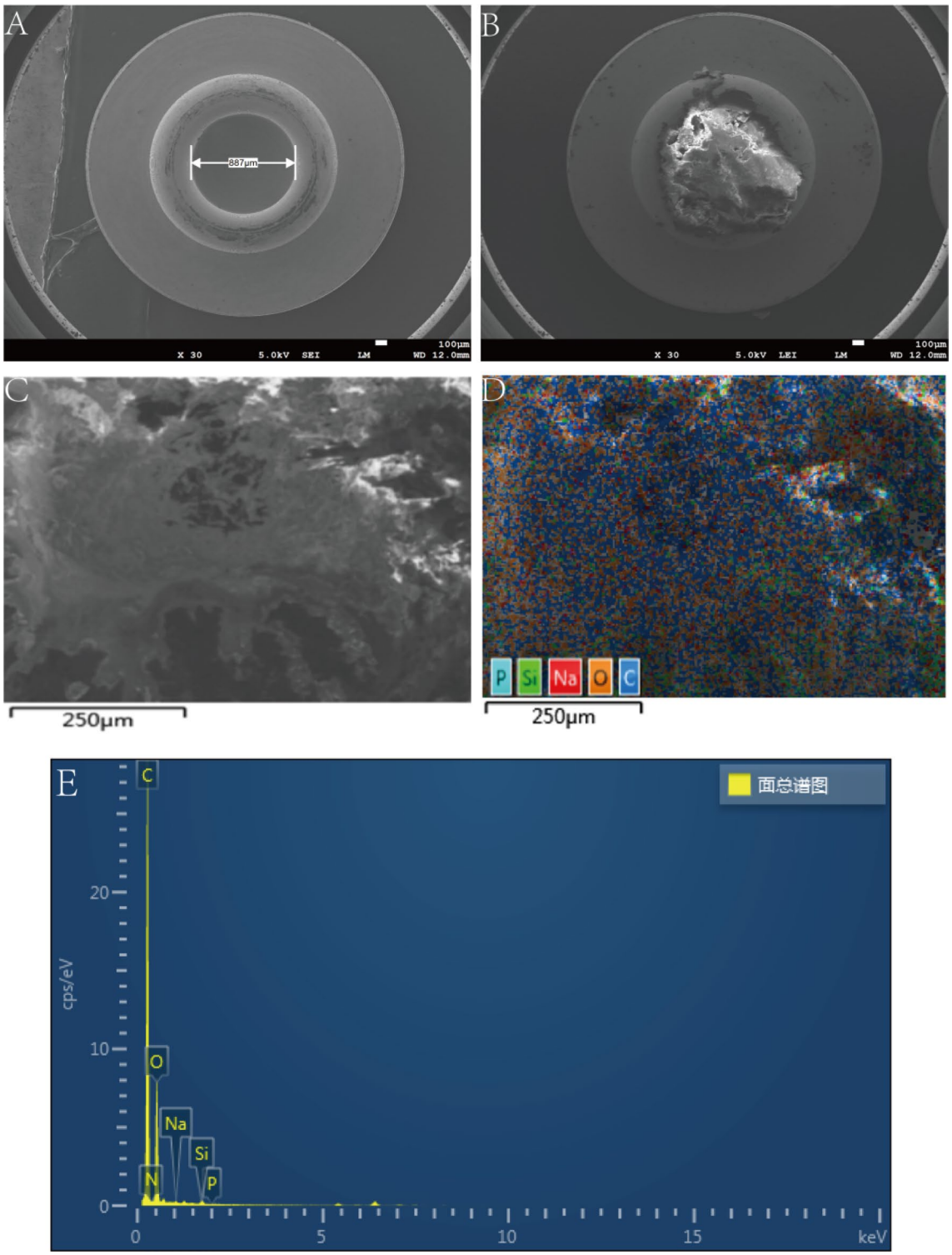

Fig. 2 **A** Leadless pacemaker electrode, **B** Leadless pacemaker electrode loaded with RAPA-PLGA, **C**–**E** EDS energy spectrum scanning surface elements of leadless pacemaker electrode loaded with RAPA-PLGA

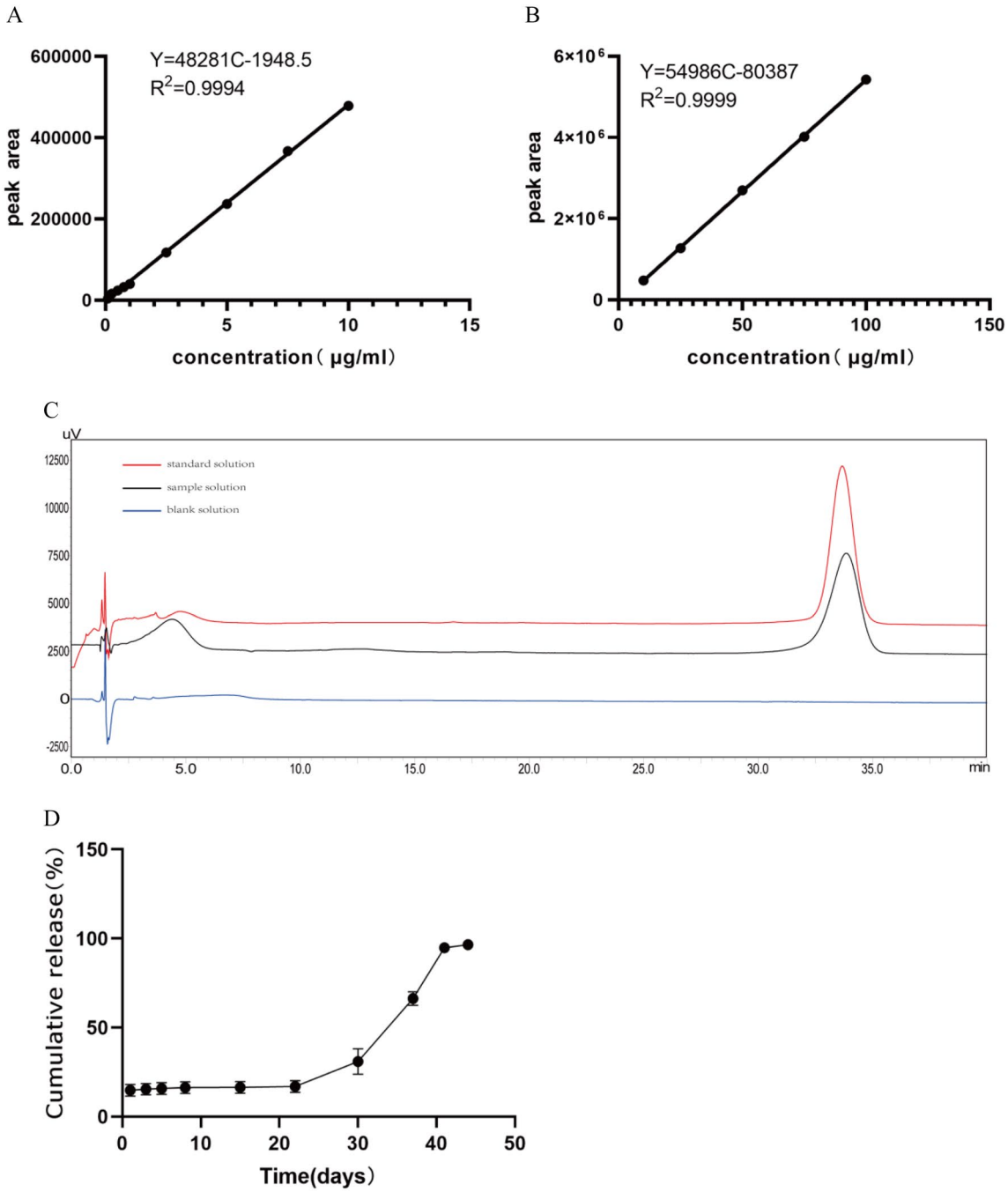

Fig. 3 RAPA detected by HPLC. **A** Standard curve for RAPA concentrations in the range of 0.1–10 μg.ml^{-1}, **B** Standard curve for RAPA concentrations in the range of 10–100 μg.ml^{-1}, **C** Overlaid chromatograms of standard solution (Red), sample solution (Blank), and blank solution (Blue), **D** In vitro release curve of LPM electrode loaded with RAPA-PLGA

Cell inhibition effect of LPM electrode loaded with RAPA-PLGA drug sustained-release system in vitro

The cell inhibition test of LPMs in vitro was conducted to compare the effect on the proliferation of the NCTC clone 929 cells before and after the electrode loaded with the RAPA-PLGA drug-sustained-release system. The cell inhibition rate was (26.29 ± 13.70) % when the cells were incubated for 48 h with the extract of the culture medium of drug-loaded electrode for 1 day; the difference between the drug-loaded electrode group and the blank electrode group was statistically significant ($P < 0.05$). The inhibition rate of the extract of drug-loaded

Table 1 Intraday precision and accuracy evaluation expressed as relative standard deviation (RSD)

Concentration (μg/mL)	Measured values (μg/mL)	Mean (μg/mL)	SD (μg/mL)	Intra-RSD (%)	Accuracy (%)
50	50.48	50.27	0.21	0.42	0.53
	50.26				
	50.07				
5	4.94	4.96	0.06	1.18	0.86
	5.02				
	4.91				
0.5	0.53	0.52	0.01	2.73	4.73
	0.51				
	0.53				

Table 2 Interday precision and accuracy evaluation expressed as relative standard deviation (RSD)

Concentration (μg/ml)	Measured values (μg/ml)	Mean (μg/ml)	SD (μg/ml)	Inter-RSD (%)	Accuracy (%)
50	50.48	48.92	1.35	2.75	2.16
	48.18				
	48.11				
5	4.94	4.81	0.14	2.83	3.87
	4.67				
	4.81				
0.5	0.51	0.52	0.01	2.67	4.06
	0.53				
	0.52				

Table 3 Test of recovery

Concentration	50 μg/ml (%)	5 μg/ml (%)	0.5 μg/ml (%)
Mean recovery ($\overline{X}$)	100.53	99.14	104.73
Standard deviation (SD)	0.42	1.17	2.86

Table 4 Quantitative stability analysis of rapamycin in release medium

Concentration (μg/ml)	Time (days)	Measured values (μg/ml)	Recovery (%)	Mean (%)	SD (%)
5	1	4.86	97.26	100.06	3.57
		4.94	98.85		
		5.20	104.08		
5	3	5.18	103.64	102.27	1.21
		5.09	101.82		
		5.07	101.34		
5	5	5.15	102.98	99.82	2.73
		4.91	98.29		
		4.91	98.20		
5	8	4.98	99.68	95.24	3.85
		4.64	92.89		
		4.66	93.15		

electrode 3 days was (38.52 ± 4.52) %. The inhibition rate reached (61.83 ± 1.05)% after the 7-day extract of the drug-loaded electrode was co-cultured with the cells for 48 h, which was significantly different from that of the blank electrode group ($P < 0.05$). With the extension of the extraction time, the inhibition effect of the cells was gradually increased, showing a specific dose–effect relationship (Fig. 4).

Effect of LPM electrode loaded with RAPA-PLGA drug sustained-release system in vivo

Local bioelectrical impedance at the implantation site of LPM electrodes

The bioelectrical impedance of different groups of mice implanted with different LPM electrodes was measured at 2 months after LPM electrode implantation. A total of 16 frequency points in the frequency range of 30,000 Hz–1000000 Hz were collected for analysis. The results showed that the muscle impedance gradually decreased from 1000000 Hz to 794,328.25 Hz, reached the lowest impedance at 794,328.25 Hz, and gradually increased from 794,328.25 Hz to 30000 Hz. The bioelectrical impedance of the implanted muscle in the LPM electrode group loaded with the RAPA-PLGA drug

Table 5 Drug loading (DL) efficiency and encapsulation efficiency (EE) measurements

Concentration (μg/ml)	DL rate(%)	Mean(%)	SD(%)	EE(%)	Mean(%)	SD(%)
120.36	48.14	51.02	2.66	80.24	85.04	4.43
128.87	51.55			85.92		
133.44	53.38			88.96		

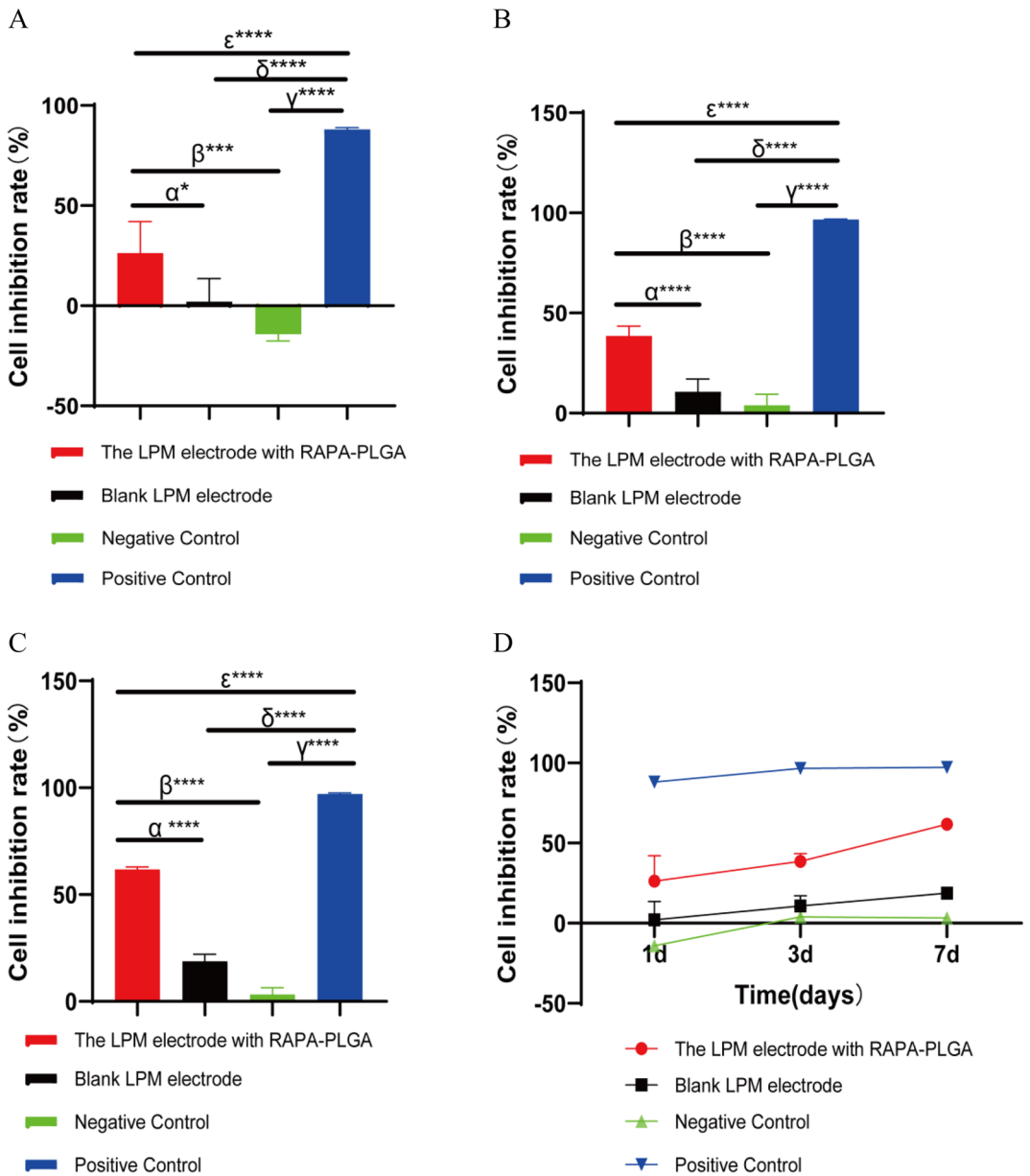

Fig. 4 Cytostatic assay of LPM electrode loaded with RAPA–PLGA. **A** Cell inhibition effect by 1-day extracts, **B** Cell inhibition effect by 3-day extracts, **C** Cell inhibition effect by 7-day extracts, **D** Overall Effect trends, α: The LPM electrode with RAPA-PLGA vs Blank LPM electrode, β: The LPM electrode with RAPA-PLGA vs Negative control, γ: Negative control vs Positive control, δ: Positive control vs Blank LPM electrode, ε: The LPM electrode with RAPA-PLGA vs Positive control, *$P < 0.05$, ***$P < 0.001$, ****$P < 0.0001$

sustained-release system was lower than that in the blank electrode group at 2 months after implantation, and the difference between the two groups was statistically significant ($P = 0.0129$) (Fig. 5C).

Pathological results at the site of LPM electrode implantation

After collecting pathological specimens from the area where electrodes are implanted, making pathological slices, and observing local pathological changes following H&E staining, the results showed that the local fibrous tissue proliferation around the LPM electrodes loaded with the RAPA-PLGA drug sustained-release system was lighter than that in the blank electrode implantation group (Fig. 5D).

Pathological results of organs

Organ specimens (including heart, liver, spleen, lungselectrodes, and kidneys) were harvested, and pathological sections were made from two experimental cohorts: (1) mice implanted with drug-sustained released electrodes and (2) mice implanted with blank electrodes. The morphological changes of organs were observed by H&E staining. The results showed that the morphology of histological pathological sections in the drug-loaded electrode group was similar to that in the control group, and the histological structure was normal. There were no obvious abnormalities in hepatocytes and cardiomyocytes. No obvious tissue damage was observed in the spleen, lung, and kidney sections (Fig. 4E), indicating that the implantation of drug-loaded electrodes did not cause damage to the organs of mice, and the safety of drug-loaded electrode implantation in vivo was preliminarily demonstrated.

Discussion

Solubility is an important physicochemical property of a compound and plays a crucial role in the bioavailability of a medication. RAPA has limited bioavailability and can easily lead to unstable medication absorption because of its highly water-insoluble nature. Consequently, in order to attain a locally effective therapeutic concentration, a high systemic dose of RAPA is required. The introduction of drug carriers provides an ideal solution for such hydrophobic drugs. The design of drug delivery systems with specific functions is the main trend in improving the therapeutic effect of drugs. In addition to its degradability, high biocompatibility, and modifiable physical and chemical characteristics, PLGA has the potential to enhance drug penetration, redistribution, and retention times in tissues, hence expanding the potential applications of hydrophobic pharmaceuticals. PLGA, as a carrier of drug microspheres, nanoparticles, micelles, etc., has been widely used in the medical field. Typically, medications were loaded via emulsification (single and double emulsion methods), microfluidic technology, electrospray technology, and spray-drying technology into PLGA [20]; the way of drug loading mainly depends on the physicochemical properties, molecular size, and preparation purpose of the drug. PLGA-loaded RAPA has also been utilized in the treatment of diseases, and emulsification is the primary process used for producing these drug-loaded particles or microspheres [21, 22]. However, such solid particles could not be stably loaded in the LPM electrode, so this study made a slight change on the basis of the above method. PLGA was emulsified by dichloromethane, followed by a specific proportion of RAPA and magnetic stirring in the fume hood to volatilize the organic solvent; the RAPA-PLGA drug sustained-release system was injected into the LPM electrode cavity when it was not fully solidified. Then, the electrodes were put in a vacuum-drying oven to allow the organic solvent to evaporate thoroughly. After that, the RAPA– PLGA sustained-release system was stable load in no pacemaker electrode.

The in vitro release kinetics and degradation rate of PLGA-loaded drugs depend not only on the solubility of drugs but also on the polymerization ratio of polylactic acid and glycolic acid in PLGA and the viscosity and molecular weight of PLGA. Choosing appropriate PLGA carrier materials can achieve different drug release effects and treatment purposes. In this study, PLGA with a viscosity of 0.38 dL/g and n (LA): n (GA) = 50:50, Mw 40,000 was used as a drug carrier. Under similar conditions, Kaamini et al. [23] showed that the drug loaded with PLGA could be released from 60 to 120 h, and the release time was different according to the molecular weight of PLGA. Amjadi et al. [24] showed that the drug release lasted for more than 20 days. Wang et al. [25] showed a sustainable release time of around 40 days, the same polymerization ratio, the sustainable release time of around 40 days, the same polymerization ratio, the larger the molecular weight, the longer the release time. In this study, the release time of LPM loaded with PLGA-RAPA lasted nearly 44 days. The lower contact surface in the release medium could be the cause of the prolonged release time in vitro. After RAPA-PLGA was placed into the LPM electrode cavity, only the RAPA-PLGA exposed at the electrode tip was completely in touch with the release medium during the release process. Subsequently, additional modifications to the viscosity, polymerization ratio, and molecular weight of PLGA can be made to extend the drug's local action period.

RAPA was prescribed at different doses to treat various illnesses. The sirolimus-eluting cobalt–chromium stent (Firebird 2) has a loading of 9 $ng.mm^{-1}$ of RAPA. ZHANG et al. [26] indicated that Firebird 2 stent can

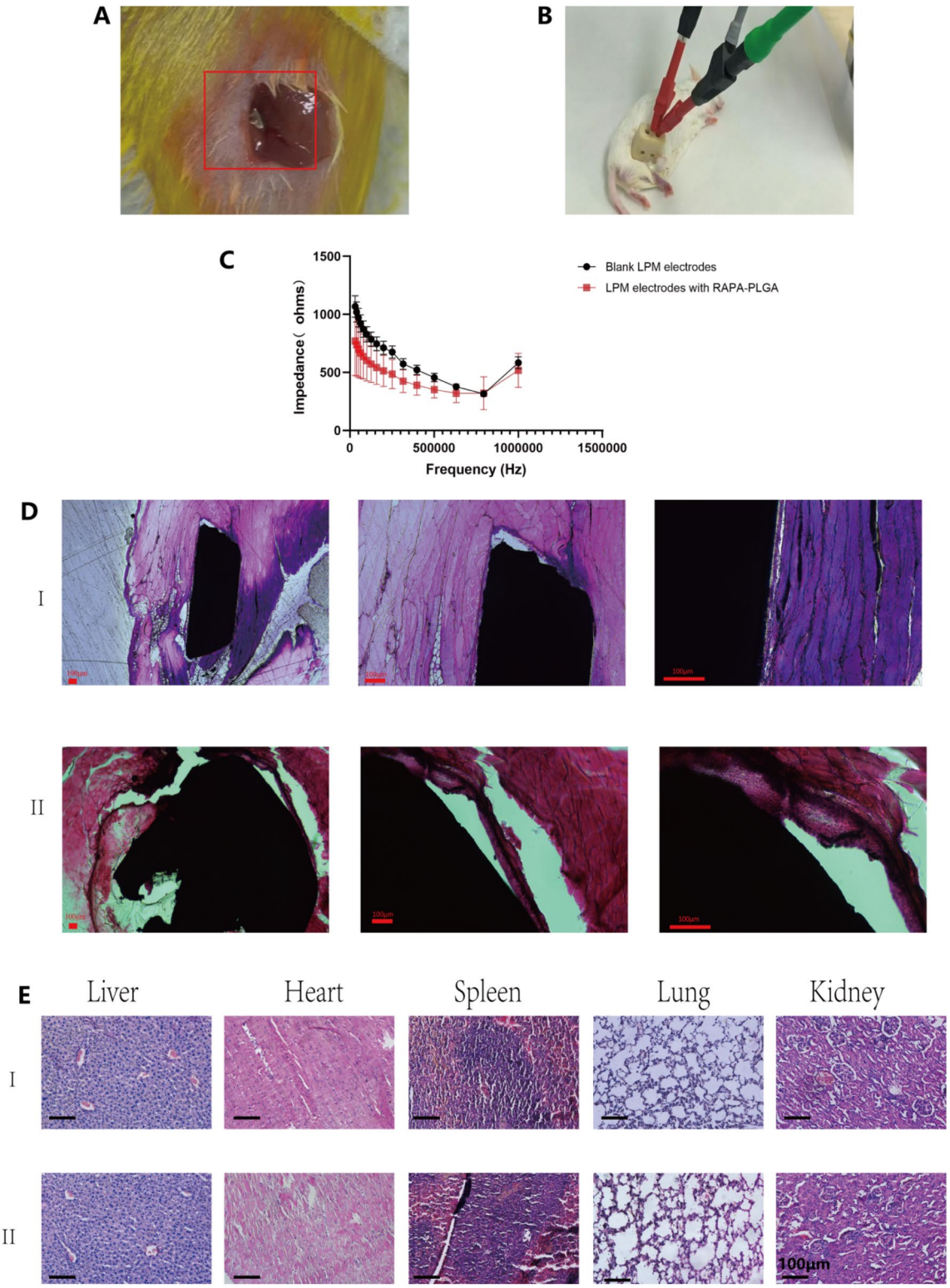

Fig. 5 Effect of LPM electrode loaded with RAPA–PLGA in vivo. **A** Implantation of LPM electrodes, **B** Determination of local bioelectrical impedance, **C** Results of local bioelectrical impedance measurements, **D** Effect of different electrodes implantation on local tissues, **E** The influence of different electrode implantation to organs, **I** The LPM electrode loaded with RAPA-PLGA implantation group, **II** Black LPM electrode implantation group,

reduce in-segment restenosis compared with conventional bare cobalt alloy stent. In terms of anti-proliferation, Ruken et al. [27] illustrated that when cultured with different concentrations of everolimus medium, the proliferation inhibition of neonatal foreskin fibroblasts (NuFF) reached the maximum level when the dose of everolimus was 40 $ng \cdot mL^{-1}$. A safe dose of 30 $ng \cdot mL^{-1}$ was chosen to impregnate the sponge; after glaucoma filtration surgery in rabbits, the region between the conjunctiva and sclera was treated for three minutes with an everolimus-impregnated sponge to determine the efficacy of RAPA in avoiding scarring. The outcomes demonstrated that, in comparison to the sham group, the local fibrous tissue density was reduced following treatment with the everolimus-impregnated sponge. Yan et al.'s study [28] also demonstrated that, in comparison to short-term sirolimus-impregnated sponge treatment, the local sirolimus-PLGA sustained-release membrane was more successful in preventing the growth of local fibrous tissue following glaucoma filtration surgery in rabbits. The amount of RAPA loaded in the LPM electrode in this investigation was approximately (337.83 ± 53.66) μg. To establish a stable release of RAPA, PLGA was loaded into the electrode to prolong the local action time of the drug. Tests for in vitro release and inhibition demonstrated that the medication inhibited the proliferation of NCTC clone 929 cells. Post-implantation, it can also effectively mitigate local fibrous tissue hyperplasia.

Bioelectrical impedance technology is a detection technology that uses the electrical properties of biological tissues and organs and their changes to extract biomedical information related to human physiological and pathological conditions. Based on the conductive differences between different tissue components of an organism, bioelectrical impedance technology is widely used in the medical field. A study [29] has shown that after myocardial ischemia, bioelectrical impedance can increase due to cell swelling and narrowing of intercellular space and later decrease due to organ death and accumulation of metabolites, indicating that bioelectrical impedance of organs can change under different conditions. Bioelectrical impedance technology can also be used to define the severity of brain tissue damage caused by external injury in rats; the more serious the tissue damage, the lower the electrical impedance [30]. Mahdavi et al. [31] used multi-frequency bioelectrical impedance technology to help define the pathological types of the marginal tissue of breast tumors. The results showed that this determination method had high accuracy, specificity, and good repeatability, indicating that bioimpedance technology can be used to define different pathological types of biological tissue. In this study, multi-frequency bioelectrical impedance was used to measure the local bioelectrical impedance of different LPM electrode implantation sites to understand the changes of local bioelectrical impedance between the control group and the electrode loaded with RAPA-PLGA drug sustained-release system group. The results showed that the bioelectrical impedance of the experimental group was lower than that of the control group, and the possible reason was that the local fibrous tissue proliferation of the control group was higher than that of the experimental group. Fibrous tissue is a denser muscle, which causes local bioelectrical impedance and increased denser muscle, thus causing local bioelectrical impedance to increase.

Conclusion

This research project innovatively developed the LPM electrode integrated with an anti-proliferative biodegradable drug sustained-release system. Initial findings indicate that this system, comprising the RAPA-PLGA drug, has the potential to mitigate local fibrous tissue proliferation and reduce local bioelectrical impedance, which provides innovative insights for alleviating local complications after LPM implantation and facilitating safe extraction following use.

Author contributions

Xiu WANG performed the experiment, data analyses and wrote the manuscript, Wentao DU helped perform the analysis with constructive discussions, Yunyun WANG assisted in the experiments, Ahsan Riaz Khan revised and verified the article, and Haijun ZHANG contributed to the conception of the study and helped perform the analysis with constructive discussions.

Funding

This study was supported by Grant No.2023YFC2411900 from the National Key Research and Development Program of China.

Data availability

No datasets were generated or analysed during the current study.

Declarations

Ethics approval and consent to participate

Not applicable.

Animal experiments and ethics

The experiment was approved by the Animal Ethics Committee of Shandong Anzhong Medical Device Inspection and Testing Co., LTD. Approval number: (2023) Scientific Research Ethics Review No. (04).

Consent for publication

The authors give full consent for publication.

Competing interests

The authors declare no competing interests.

Author details

[1]College of Clinical Medicine, Hebei University of Engineering, Handan 056000, China. [2]Department of Cardiovascular Medicine, Affiliated Hospital of Hebei Engineering University, Handan 056000, Hebei, China.

[3]Department of Interventional and Vascular Surgery, Shanghai Tenth People's Hospital, Tongji University School of Medicine, Shanghai 200072, China. [4]National United Engineering Laboratory for Biomedical Material Modification, Branden Industrial Park, Qihe Economic & Development Zone, Dezhou 251100, Shandong, China. [5]School of Medicine, Tongji University, Shanghai 200000, China.

Received: 7 December 2024 Accepted: 18 April 2025
Published online: 30 April 2025

References

1. Ngo L, Nour D, Denman RA, et al. Safety and efficacy of leadless pacemakers: a systematic review and meta-analysis. J Am Heart Assoc. 2021;10(13): e019212.
2. Piccini JP, El-Chami M, Wherry K, et al. Contemporaneous comparison of outcomes among patients implanted with a leadless vs transvenous single-chamber ventricular pacemaker. JAMA Cardiol. 2021;6(10):1187–95.
3. Kypta A, Blessberger H, Kammler J, et al. First autopsy description of changes 1 year after implantation of a leadless cardiac pacemaker: unexpected ingrowth and severe chronic inflammation. Can J Cardiol. 2016;32(12):1578.e1571-1578.e1572.
4. Breeman KTN, du Long R, Beurskens NEG, et al. Tissues attached to retrieved leadless pacemakers: histopathological evaluation of tissue composition in relation to implantation time and complications. Heart Rhythm. 2021;18(12):2101–9.
5. Klawitter J, Nashan B, Christians U. Everolimus and sirolimus in transplantation-related but different. Expert Opin Drug Saf. 2015;14(7):1055–70.
6. Moes DJ, Guchelaar HJ, de Fijter JW. Sirolimus and everolimus in kidney transplantation. Drug Discov Today. 2015;20(10):1243–9.
7. Andrade DL, Jalalizadeh M, Salustiano ACC, et al. Bladder cancer immunomodulatory effects of intravesical nitazoxanide, rapamycin, thalidomide and Bacillus Calmette-Guérin (BCG). World J Urol. 2023;41(9):2375–80.
8. O'Shea AE, Valdera FA, Ensley D, et al. Immunologic and dose dependent effects of rapamycin and its evolving role in chemoprevention. Clin Immunol. 2022;245: 109095.
9. Bae IH, Lim KS, Park DS, et al. Sirolimus coating on heparinized stents prevents restenosis and thrombosis. J Biomater Appl. 2017;31(10):1337–45.
10. Buss SJ, Muenz S, Riffel JH, et al. Beneficial effects of mammalian target of rapamycin inhibition on left ventricular remodeling after myocardial infarction. J Am Coll Cardiol. 2009;54(25):2435–46.
11. Yu SY, Liu L, Li P, et al. Rapamycin inhibits the mTOR/p70S6K pathway and attenuates cardiac fibrosis in adriamycin-induced dilated cardiomyopathy. Thorac Cardiovasc Surg. 2013;61(3):223–8.
12. Gomez-Manjarres DC, Axell-House DB, Patel DC, et al. Sirolimus suppresses circulating fibrocytes in idiopathic pulmonary fibrosis in a randomized controlled crossover trial. JCI Insight. 2023;8(8): e166901.
13. Neef M, Ledermann M, Saegesser H, et al. Low-dose oral rapamycin treatment reduces fibrogenesis, improves liver function, and prolongs survival in rats with established liver cirrhosis. J Hepatol. 2006;45(6):786–96.
14. Chen G, Chen H, Wang C, et al. Rapamycin ameliorates kidney fibrosis by inhibiting the activation of mTOR signaling in interstitial macrophages and myofibroblasts. PLoS ONE. 2012;7(3): e33626.
15. Guo X, Zuo X, Zhou Z, et al. PLGA-based micro/nanoparticles: an overview of their applications in respiratory diseases. Int J Mol Sci. 2023;24(5):4333.
16. Hashemi M, Shamshiri A, Saeedi M, et al. Aptamer-conjugated PLGA nanoparticles for delivery and imaging of cancer therapeutic drugs. Arch Biochem Biophys. 2020;691: 108485.
17. Cappellano G, Comi C, Chiocchetti A, et al. Exploiting PLGA-based biocompatible nanoparticles for next-generation tolerogenic vaccines against autoimmune disease. Int J Mol Sci. 2019;20(1):204.
18. Pinto M, Silva V, Barreiro S, et al. Brain drug delivery and neurodegenerative diseases: polymeric PLGA-based nanoparticles as a forefront platform. Ageing Res Rev. 2022;79: 101658.
19. Jiao-miao P, Xiao-yan X, Bei L, et al. Preparation and in vitro release study of rapamycin in poly(lactic-co-glycolic)acid microsphere for topical administration. Chin J Aesthet Med. 2010;19(03):334–7.
20. Su Y, Zhang B, Sun R, et al. PLGA-based biodegradable microspheres in drug delivery: recent advances in research and application. Drug Deliv. 2021;28(1):1397–418.
21. Dhanabalan KM, Dravid AA, Agarwal S, et al. Intra-articular injection of rapamycin microparticles prevent senescence and effectively treat osteoarthritis. Bioeng Transl Med. 2023;8(1): e10298.
22. Zhao R, Zhu M, Zhou S, et al. Rapamycin-loaded mPEG-PLGA nanoparticles ameliorate hepatic steatosis and liver injury in non-alcoholic fatty liver disease. Front Chem. 2020;8:407.
23. Dhanabalan KM, Gupta VK, Agarwal R. Rapamycin-PLGA microparticles prevent senescence, sustain cartilage matrix production under stress and exhibit prolonged retention in mouse joints. Biomater Sci. 2020;8(15):4308–21.
24. Amjadi I, Rabiee M, Hosseini MS, et al. Synthesis and characterization of doxorubicin-loaded poly(lactide-co-glycolide) nanoparticles as a sustained-release anticancer drug delivery system. Appl Biochem Biotechnol. 2012;168(6):1434–47.
25. Wang J, Helder L, Shao J, et al. Encapsulation and release of doxycycline from electrospray-generated PLGA microspheres: effect of polymer end groups. Int J Pharm. 2019;564:1–9.
26. Zhang Q, Xu B, Yang YJ, et al. Sirolimus-eluting cobalt alloyed stents in treating patients with coronary artery disease: six-month angiographic and one-year clinical follow-up result. A prospective, historically controlled, multi-center clinical study. Chin Med J (Engl). 2007;120(7):533–8.
27. Cinik R, Yüksel N, Pirhan D, et al. The effect of everolimus on scar formation in glaucoma filtering surgery in a rabbit model. Curr Eye Res. 2016;41(11):1438–46.
28. Yan ZC, Bai YJ, Tian Z, et al. Anti-proliferation effects of Sirolimus sustained delivery film in rabbit glaucoma filtration surgery. Mol Vis. 2011;17:2495–506.
29. Gersing E. Impedance spectroscopy on living tissue for determination of the state of organs. Bioelectrochem Bioenerg. 1998;45(2):145–9.
30. Harting MT, Smith CT, Radhakrishnan RS, et al. Regional differences in cerebral edema after traumatic brain injury identified by impedance analysis. J Surg Res. 2010;159(1):557–64.
31. Mahdavi R, Hosseinpour P, Abbasvandi F, et al. Bioelectrical pathology of the breast; real-time diagnosis of malignancy by clinically calibrated impedance spectroscopy of freshly dissected tissue. Biosens Bioelectron. 2020;165: 112421.

Publisher's Note